The ultrasonic grinding process temperature field study

Alexander Unyanin[1] and *Albert* Khusainov[2,*]

[1]Ulyanovsk State Technical University, Department of Machine Building, 432027, Sev. Venec, 32, Ulyanovsk, Russia
[2] Ulyanovsk State University, Department of Physics and Engineering, 432017, L. Tolstoy, 42, Ulyanovsk, Russia

Abstract. The use of ultrasonic energy is a promising way to improve the efficiency of the grinding process. However, the analytical study of local temperatures during ultrasonic grinding was not performed. In the process of research, physical and mathematical models have been developed for calculating the temperature field during grinding, taking into account the change of the kinematics of microcutting by abrasive grains and the change of the mechanical characteristics of the workpiece material when ultrasonic vibrations are applied. The models take into account that the parameters, characterizing the workpiece material resistance to dispersing, and the thermophysical properties of abrasive grain, workpiece, chips and external environment, depend on the temperature. The modeling was performed on the basis of a simultaneous solution of the thermal conductivity differential equations, written for each interacting object. For equation calculation the finite-element method was used. The methodology and software for the temperature field calculation have been developed. The temperature modeling results are shown. The effect of the vibration amplitude and phase on the local temperatures in the area of abrasive grain, chips and workpiece contact, including the grain and the workpiece contact time, has been determined. The factors affecting the local temperatures have been determined. During ultrasonic activation the workpiece temperature is lowered by 10 %, and the local temperatures in the abrasive grain, workpiece and chips contact area are lowered by 30 %.

1 Introduction

Grinding wheel performance improvement and treated parts quality improvement while ultrasonic grinding are largely due to this process thermal intensity change [1-3]. However, the analytical study of the temperature field while ultrasonic grinding was not performed.

The thermal processes in grinding are studied sufficiently well [4-6], but in most analytical studies the grinding wheel and the workpiece contact area represents a solid thermal source and the average contact temperatures are calculated. Local temperatures must be known in order to assess the grinding wheel working conditions and the quality parameters of the grinded workpiece thin surface layer [7-9].

The aim of the study is to determine the ultrasonic vibration parameters affecting the temperature field of the grinding process.

For achieving the aim the following problems were solved:
– physical and mathematical models development for the temperature field calculation;
– numerical modeling methodology and software development for the temperature field calculation;
– temperatures numerical modeling and the analysis of the obtained results.

2 Study Methodology

Consideration has been given to heat release in the area of the workpiece material deformation with the abrasive grain and in the areas of grain contact with chips *NE* and the workpiece *EV* (the densities of the heat release sources are q_{∂}, q_{1T}, q_{2T}, respectively) (Figure 1). It was assumed that the source of q_{∂} density was evenly distributed, and the sources of q_{1T} and q_{2T} density were distributed by antisymmetric normal and exponential law, respectively [9-11]. The components of the microcutting force, the power and the thermal sources density were calculated by the analytic dependences [9, 10]. For example, the heat release density in the grain and the workpiece contact area at the distance of x from the point E (see Figure 1) may be calculated as follows

$$q_{2T}(x) = q_{2T} \cdot \exp\left[-k_0 \cdot x\right]; \quad (1)$$

$$q_{2T} = \frac{W_{2T} \cdot k_0}{l_2 \cdot \exp\left[-k_0 \cdot l_2\right]};\ W_{2T} = \frac{\mu_o \cdot \tau_s \cdot f_t \cdot V_K}{3\mu_s}, \quad (2)$$

where k_0 is coefficient, m^{-1}; f_t is a surface area of the grain friction against the workpiece, m^2; μ_s is an internal friction coefficient [12]; l_2 is a size of the site dullness on the grain, m; τ_s are shear stresses, Pa [12-14]; μ_0 is a coefficient of the grain friction against the workpiece; V_K is a working speed of the grinding wheel, m/s; W_{2T} is a heat release power, W.

* Corresponding author: a.s.khusainov@gmail.com

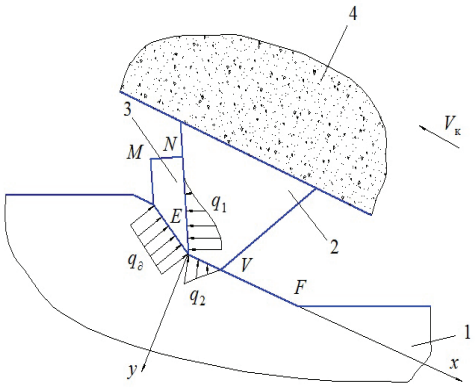

Fig. 1. The scheme for the heat exchange calculation in the grain and the workpiece contact area: 1 – workpiece; 2 – grain; 3 – chips; 4 – grinding wheel

The abrasive grain is presented as a truncated pyramid, the chips and the workpiece are presented as the cuboids [5, 9]. To improve the accuracy of the results, the dependences of the parameters characterizing the workpiece material resistance to dispersing [14, 15] are taken into account, and the dependences of the thermophysical properties of all the interacting objects (including the external environment objects) on the temperature are also considered. The modeling was performed on the basis of a simultaneous solution of the thermal conductivity differential equations, written for each interacting object, and considering the speed of their relative displacement (of the grain in relation to the workpiece and of the chips in relation to the grain).

To consider the temperature field formation as a result of pile-up of thermal pulses from separate grains, displacement (see Figure 1) of a series of the grains successively contacting with the workpiece was modeled.

When flat grinding without ultrasonic vibrations the depth of the cutting grain penetration into the workpiece material depending on the distance l, covered by the grain on the trajectory of contact with the workpiece (Curve 1 in Figure 2), is described by the dependency

$$a(l) = a_k + A \cdot l\,, \tag{3}$$

where a_k is a critical microcutting depth, m; A is a coefficient [9, 10].

When there is the workpiece vibration in the direction which is perpendicular to its processed surface (see Figure 2), the depth of the cutting grain penetration into the workpiece may be presented as follows

$$a_1(l) = a(l) + A_u \cdot sin(\omega \frac{l}{V_K} + \varphi), \tag{4}$$

where A_u is the amplitude of the workpiece vibration in the direction which is perpendicular to the processed surface, m; ω is a vibrations cyclic (circular) frequency, rad/c; φ is an ultrasonic vibration phase, rad.

When ultrasonic vibrations take place on a part of the trajectory of contact with the workpiece, the grind will have a greater penetration depth than that without vibrations; on the other part of a contact the penetration depth is less (see Figure 2).

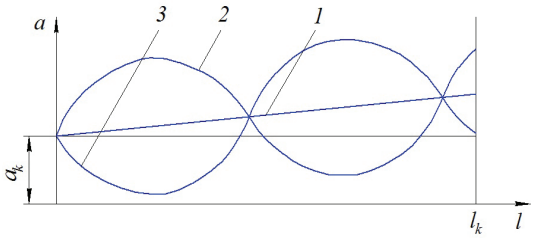

Fig. 2. Dependence of the depth of the grain penetration into the workpiece a on the distance l covered by the grain on the contact trajectory: 1 – without vibrations; 2, 3 – with the workpiece vibration with the phase φ = 0° and 180°, respectively

The workpiece vibration with ultrasonic frequency results in a qualitative change of the process of its material dispersing by the abrasive grains of the grinding wheel. Ultrasonic activation is accompanied by the workpiece material ultimate strength and fluidity reduction and the reduction of its ability for hardening in the deformation process [1].

The average sheer stresses by sheer area, defining the grinding wheel grains microcutting force,

$$\tau_S = \frac{\sigma_в \cdot 1{,}558 \cdot e^{2{,}34 \cdot 10^{-3} \cdot T}}{\sqrt{3}}, \tag{5}$$

where $\sigma_в$ is a workpiece material temporary resistance, Pa [14, 16]; T is a workpiece material deformed layer temperature, K. The ultrasonic activation of the workpiece results in the reduction of $\sigma_в$ by 10 … 15 % [1].

The thermal conduction differential equations of the objects (grain, workpiece, grinding wheel and chips) were solved in conjunction with the general boundary conditions in the contact area, which allows to consider the thermal flows distribution between the objects. For example, in the limits of a contact of the workpiece 1 with the grain 2 (see Figure 1) the surface interaction conditions are described by the following boundary conditions:

$$\frac{\partial T_1}{\partial y} = -\frac{q'_{2T}}{\lambda_1};\ \frac{\partial T_2}{\partial y} = -\frac{q''_{2T}}{\lambda_2};\ T_1 = T_2; \tag{6}$$

$$q'_{2T} + q''_{2T} = q_{2T}\,, \tag{7}$$

where T_1 and T_2 are the workpiece and the grain temperatures in the contact area; λ_1, λ_2 are the workpiece and the grain materials conductivity coefficients, W/(mK); q'_{2T}, q''_{2T} are the density of the thermal flows into the workpiece and the grain, respectively.

Heat exchange at the boundaries of the objects, which contact with the process liquid and air, is set in the form of Newton-Richmann law describing the convective heat exchange process as

$$-\lambda_z \frac{\partial T_z}{\partial n} = \alpha_j \cdot (T_z - T_0), \qquad (8)$$

where z is an object number (z = 1, 2, 3, 4 for the workpiece, the grain, the chips and the grinding wheel, respectively); j is a surface number; α_j is a heat transfer coefficient from j surface, W/(m^2·K).

The finite-element method was used for the conductivity differential equations calculation [17]. Numerical procedure on the basis of the conductivity equations discrete analogs is implemented in the original programs.

The adequacy to the real conditions of the physical and mathematical models adopted while temperatures calculation was tested by comparing the average contact temperature experimental values while ultrasonic grinding of the workpieces made of stainless steel 12X18H9T with the calculation values. The difference between the calculation and experimental values does not exceed 26 %, that indicates the possibility of using the method for the thermophysical analysis of the grinding process.

For conducting of the experimental studies an experimental plant, based on the face-grinding machine and equipped with the ultrasonic device, has been developed [18, 19]. The workpiece is one of the vibration system links and is attached between the vibrations source and the reflector. The total length of the vibrations source, the workpiece and the support is equal to the ultrasonic vibration wave length, that is why the workpiece has a maximum vibrations amplitude. The ultrasonic vibration minimum energy losses and the workpiece vibrations high amplitude are also achieved by the adequate contact of the vibrations source with the workpiece that is provided while attaching it.

Experimentally, it has been established that, with the vibrations amplitude in the direction perpendicular to the workpiece processed surface A_u exceeding 3 μm, the grinding wheel wear intensity and the height parameters of the processed surface microgeometry increase. Therefore, while modeling and experimental temperature study the amplitude A_u was limited to 3 μm.

The numerical temperature modeling was performed by the following source data: multipass flat grinding with the grinding wheel face; the workpiece material is steel 40X and 12X18H9T; the grinding wheel grains material is Brown Aluminium Oxide 24A and borazon; Brown Aluminium Oxide graininess is *F*60 (25-th); the grinding wheel operating speed V_K = 35 … 70 m/s; traverse speed V_S = 10 m/min; grinding depth t = 0,01 mm. The ultrasonic activation of the workpiece with various amplitudes and phases was modeled with the ultrasonic vibration frequency of 18600 Hz. The local temperatures on the grain and the workpiece contact site *EV* and the grain and the chips contact site *NE*, and also the workpiece surface layers temperature were recorded.

3 Study Results and Discussion

The results of modeling when processing the workpieces made of steel 40X with Brown Aluminium Oxide wheel, are presented below. At the vibrations amplitude A_u = 1 μm the temperature T_2 in the area of the grain and the workpiece contact was lower by 8 ... 9 %, the temperature T_2' in the area of the grain and the chips contact was lower by 8 ... 14 %. With ultrasonic vibrations with the amplitude A_u = 2 μm the local temperatures decreased to a greater extent: the temperature T_2 decreased by 9 ... 14 %, T_2' decreased by 17 ... 31 % (Figures 3, 4).

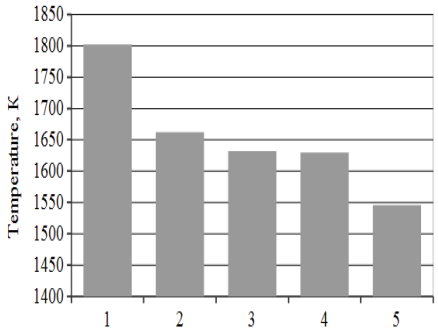

Fig. 3. The temperature T_2 in the area of the grain and the workpiece contact: 1 – A_u = 0 (without ultrasonic vibration); 2 – A_u = 1 μm, φ = 0°; 3 – A_u = 1 μm, φ = 180°; 4 – A_u = 2 μm, φ = 0°; 5 – A_u = 2 μm, φ = 180°.

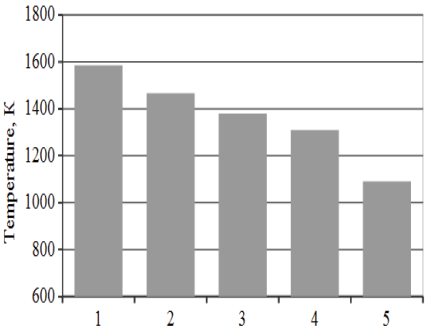

Fig. 4. The temperature T_2' in the area of the grain and the chips contact: 1 – A_u = 0 (without ultrasonic vibration); 2 – A_u = 1 μm, φ = 0°; 3 – A_u = 1 μm, φ = 180°; 4 – A_u = 2 μm, φ = 0°; 5 – A_u = 2 μm, φ = 180°.

Local temperatures are significantly dependent on the ultrasonic vibration phase, with lower temperatures being recorded during the phase φ = 180°. The obtained result may be explained by the fact that during this phase the minimum length of the trajectory, where the grain performs the workpiece microcutting, takes place. In this case, the grain does not perform microcutting at the greater trajectory part, that causes the process thermal power intensity decrease. The maximum cutting trajectory length is obtained with φ = 0°; therefore, at this trajectory the high temperatures are recorded. The microcutting trajectories lengths and the local temperatures with the phases 90° and 270° have intermediate values.

The temperature difference during various phases is as more as the ultrasonic vibration amplitude is higher. In the case of A_u = 1 μm, the difference in temperatures T_2 with the phases φ = 0° and φ = 180° is 2 %, in temperatures T_2' is 6 %; at A_u = 2 μm this difference is 5 and 15 %, respectively (see Figures 3, 4).

In the case of grinding without ultrasonic vibrations, the local temperatures increase with the increase of the workpiece and the grain contact duration (Figures 5, 6, Curve 1). With ultrasonic activation with the phase φ = 0° in the initial contact period the grain penetration depth into the workpiece is higher, and at the trajectory end is lower than without ultrasonic activation (see Figure 2). Accordingly, the local temperatures in the initial period of contact with the workpiece are slightly lower than at A_u = 0 (Curves 1 and 2 in Figures 5, 6). At the final stage of the grain contact with the workpiece the temperature difference is significantly higher, as the penetration depth is lower.

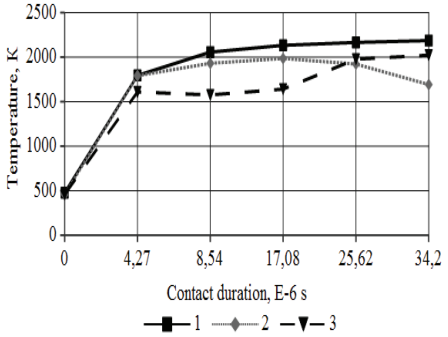

Fig. 5. Dependence of the temperature T_2 in the area of the grain and the workpiece contact on the contact duration: 1 – A_u = 0; 2 – A_u = 2 μm, φ = 0°; 3 – A_u = 2 μm, φ = 180°.

With the vibrations phase φ = 180° in the initial period of contact both the depth of the grain penetration into the workpiece and the local temperatures are lower than they are while grinding without ultrasonic vibrations (Curves 1 and 3 in Figures 5, 6). In particular, at the time moment of the grain contact with the workpiece τ = 8,54·10^{-6} s the temperature T_2 is lower by 23 %, T_2' is lower by 3.25 times. At the final stage the depth of the grain penetration into the workpiece with ultrasonic vibrations with the phase φ = 180° increases, so, the temperatures also increase; however, at this stage the temperatures are lower than they are when grinding without ultrasonic vibrations.

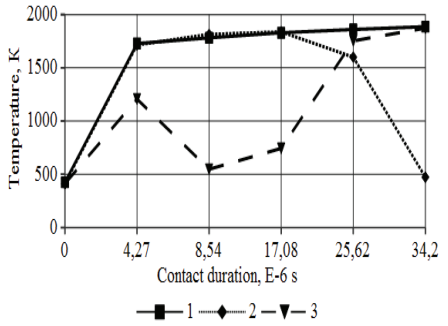

Fig. 6. The dependence of the temperature T_2' in the grain and the chips contact area on the contact duration: 1 – A_u = 0; 2 – A_u = 2 μm, φ = 0°; 3 – A_u = 2 μm, φ = 180°.

On the site of the grain contact with the workpiece the temperature is unevenly distributed (Figure 7). The maximum temperature is recorded at a distance of 5 ... 10 μm from the top of the grain (point *E* in Figure 1).

The average workpiece temperature at a distance of 2 and 100 μm from its surface and the workpiece material deformed layer temperature with ultrasonic vibrations were lower by 9 ... 11 %, whereas the vibrations amplitude only slightly affects these temperatures (Figure 8). Ultrasonic vibrations are more likely to affect the temperature in the workpiece surface layers than the temperature at a distance from this surface (Figure 9).

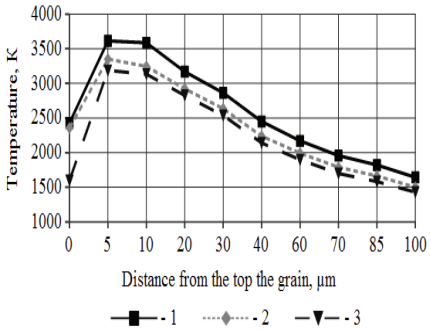

Fig. 7. The temperature distribution on the site of the grain contact with the workpiece: 1 – A_u = 0; 2 – A_u = 2 μm, φ = 0°; 3 – A_u = 2 μm, φ = 180°.

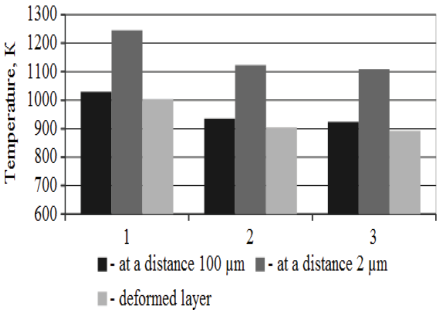

Fig. 8. The workpiece temperature: 1 – A_u = 0; 2 – A_u = 1 μm; 3 – A_u = 2 μm.

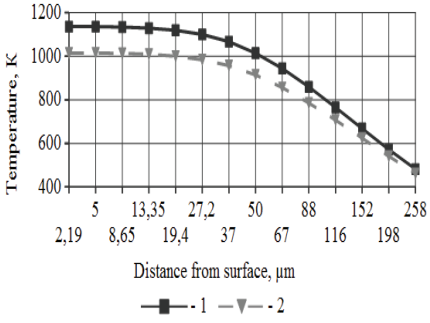

Fig. 9. The workpiece temperature distribution: 1 – A_u = 0; 2 – A_u = 2 μm.

Using the grinding wheels made of borazon provides lower local temperatures (by 1.5 times) and workpiece temperatures (more than twice), compared to using the grinding wheels made of the Brown Aluminium Oxide at the same mode. The reason is the higher borazon thermal conductivity coefficient, the smaller size of the site dullness on the grains and the greater distance between the cutting grains, thus the workpiece surface layer gets cold to lower temperatures.

When the operating speed of the borazon grinding wheel increases due to the heat release sources power

increase, the local temperatures also increase. When grinding without ultrasonic vibrations with the speed increase from 35 to 70 m/s, the temperature in the area of the grain contact with the workpiece and with the chips increases by 13 and 26 %, respectively. With ultrasonic vibrations with the amplitude of 2 μm not exceeding the depth of the grain penetration into the workpiece (the grain does not lose the contact with the workpiece during ultrasonic activation), the temperatures in the area of the grain contact with the workpiece and the chips were lower than those without ultrasonic vibrations by 12 and 15 % at the grinding wheel speed of 35 m/s, and by 13 and 17 % at the speed of 70 m/s. Consequently, with the grinding wheel speed increase, the ultrasonic vibrations provide the slightly greater temperature drop. With ultrasonic vibrations with the amplitude of 3 μm exceeding the depth of the grain penetration into the workpiece (the grain loses the contact), the temperatures were reduced by almost 2 times.

4 Main results and conclusions

1. The ultrasonic vibrations during grinding allow to reduce the temperature in the workpiece surface layers to 10 %, the local temperatures in the area of the grain contact with the workpiece and the chips – to 13 and 30 %, respectively.
2. The temperature decrease is mainly affected by change of the stressed and strained state in the processing area due the workpiece material strength specifications reduction and the change of the microcutting kinematics during ultrasonic vibrations;
3. The effect of the ultrasonic vibration amplitude and phase on the temperature field and the effect of ultrasonic vibration parameters on the local temperatures are established, depending on the duration of the grain and the workpiece contact.

References

1. M. F. Vologin, V. V. Kalashnikov, M. S. Nerubai, B. L. Shtrikov, *Application of ultrasound and explosion during processing and assembly* (2002)
2. C. Guo, S. Malkin, Trans. ASME. J. Eng. Ind., **117 (4)**, 571 – 577 (1995)
3. J. Ja, J. Kim, Ju. Sun, J. Jang, Trans. ASME. J. Manuf. Sci and Eng., **121 (3)**, 378 – 384 (1999)
4. D. G. Evseev, A. N. Salnikov, *Physical basis of the grinding process* (1978)
5. A. N. Reznikov, L. A. Reznikov, *Thermal processes in technological systems* (1990)
6. A. V. Yakimov, P. T. Slobodnyak, A. V. Usov, *Thermophysics of mechanical processing* (1991)
7. A. N. Unyanin, STIN, **1**, 28 – 32 (2006)
8. L. V. Khudobin, A. N. Unyanin, Russian Engineering Research, **28 (9)**, 913 (2008)
9. L. V. Khudobin, A. N. Unyanin *Minimizing the loading of grinding wheels* (2007)
10. A. N. Unyanin, Izvestiya vuzov. Mashinostroenie, **6**, 41 – 50 (2006)
11. A. N. Unyanin, Russian Engineering Research, **29 (6)**, 630 - 632 (2009)
12. V. V. Efimov, *Model of grinding process using coolant* (1992)
13. L. N. Filimonov, *Resistance of grinding wheels* (1973)
14. S. N. Korchak, *Performance of grinding process of steel parts* (1974)
15. A. A. Diakonov, Izvestiya vuzov. Mashinostroenie, **7**, 60 – 62 (2007)
16. V. A. Nosenko, *Grinding of adhesion-active metals* (2000)
17. D. Shi, *Numerical methods in heat transfer problems* (1988)
18. A. N. Unyanin, I. Yu. Terekhin, Patent RU 2418671 RF, IPC B 24 B 1 / 04, B 24 B 5 / 04, **14** (2011)
19. A. N. Unyanin, A. S. Khusainov, Procedia Engineering, **150**, 1000 – 1006 (2016).